International Conference on Green Energy & Environmental Engineering (GEEE-2018)
Proceedings of Engineering and Technology – PET
Vol.37 pp.19-24

Sliding Mode Control of An Autonomous Sailboat

Helmi Abrougui[1], Samir Nejim[2]
U.R Automatic Control & Marine Robotics
Naval Academy, Tunisia
[1]helmiabrougui@yahoo.fr
[2]samir.nejim@centraliens.net

***Abstract*:—This paper presents a study on the development of an autopilot based on sliding mode method for a sailing vessel. This autopilot is synthesized through a model with three degrees of freedom, which represents the dynamics of the boat. The dynamic equations of motion are strongly nonlinear. However, we will design control laws to stabilize the boat heading and sail opening angle in order to make it follow a given path. We first describe the nonlinear three-degree-of-freedom dynamic model for the sailing vessel. Then, we design an autopilot using sliding mode techniques. Finally, some simulations are carried out to illustrate the behaviour of the overall system.**

Keywords—autonomous sailboat; autopilot; sliding mode control.

I. INTRODUCTION

Due to their low energy consumption, robotic sailing boats offer a promising solution for observation or monitoring missions at sea. Actually, many autonomous sailboat projects have been launched throughout the world over the last decade [3].

Generally, the sailboat propulsion depends on the wind. Even though this propulsive resource is free and environment friendly, its major disadvantage resides in the uncontrollability and unpredictability of the wind. Hence, we need an effective adjustment of the sail and the rudder angle to overtake this weakness. This adjustment must be effective to control the sailboat heading and the sail opening angle. For this purpose, it will be necessary to determine a dynamic model of the sailboat. In this context, several approaches have been developed. Actually, the classical techniques of Lagrangian and Newtonian mechanics are the most used methods for modelling the behaviour of the sailboat in the presence of the different efforts applied to the boat. In this context, two types of dynamic models are distinguished, those of three degrees of freedom with no drift effect, especially announced in [6], and those with drift effect highlighted in [13]. Also, other examples of developed dynamic models are presented in [13 and 14]. In [8] Legursky determined also a 4-DOF[1] sailboat dynamic model using another approach with a modification in the aerodynamic effort.

To ensure an effective and safety navigation of autonomous sailboats, several control laws have been applied. In [1], Brière developed a linear controller to calculate the sail opening angle as a function of the apparent wind angle. Another controller based on fuzzy logic techniques has been developed in [15] and [10] to ensure an optimal roll angle of the sailboat. In 2010, a controller based on extremum-seeking was proposed by Jouffroy in order to calculate the optimal control of the sail and to maximize the boat linear velocity [11].

To guide the sailboat to its destination, an appropriate control of the rudder angle must be achieved. The most used regulators are the PID correctors (see [2] and [9]). This command is synthesized according to the modelling of the sailboat rotation with the first order Nomoto model. Another fuzzy-based controller has been established by Gomes [16] where the rudder angle was calculated using the heading and the desired angular velocity. Moreover, a back-stepping approach was introduced by Jouffroy [13] to design a nonlinear rudder controller.

In this paper, an autopilot was designed using sliding mode techniques for controlling the rudder and the sail opening angle in the same time letting the sailboat follow a given path.

In the following section, before the design of control laws are presented, a mathematical model of a sailboat with three degrees of freedom was described. In section III, the sail and heading controller were applied and tested on the presented model. Finally, some simulations were carried out to illustrate the approach.

II. SAILBOAT DYNAMIC MODEL

In this paper our objective is to design an autopilot for controlling the heading and sail opening angle of the sailing

This work was supported by the "Ministry of Higher Education and Scientific Research (MESRST)"

[1] Degrees of freedom

ISSN 2356-5608

boat. Firstly, the nonlinear 3-DOF dynamic model for the sailing vessel is described. This model is inspired from [5] under the following assumptions:

- The wind speed and direction are constant.
- Rolling motion and drift effect are neglected.
- The boat is assumed to be rigid with 3 DOFs: surge, sway and yaw. (see Appendix B)
- The sailboat is assumed to evolve in calm waters.
- The environmental disturbances are ignored.

The figure (Fig.1) shows the sailing boat to be modeled.
Let the North-East-Down NED coordinate system (x, y, z) be the inertial reference frame $(n-frame)$ and let the (x_b, y_b, z_b) be the body fixed frame $(b-frame)$(Fig.1). The latter is the rotating reference frame attached to the boat with yaw velocity $\dot{\psi} = r$ relative to the $(n-frame)$.

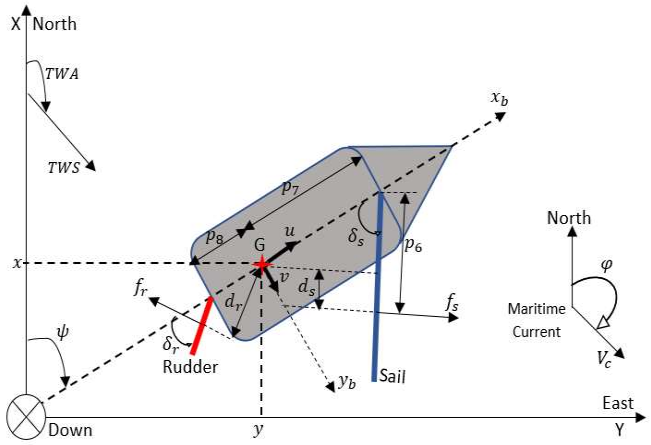

Fig. 1. Graphic representation of the modelled sailboat and Description of the (b-frame) coordinate system

The kinematic equations are:

$$\dot{x} = u\cos\psi + V_C\cos\varphi \quad (1)$$

$$\dot{y} = u\sin\psi + V_C\sin\varphi \quad (2)$$

$$\dot{\psi} = r \quad (3)$$

According to [5] and [17], the wind generates an aerodynamic force on the sail which is equal to:

$$f_s = p_4(V_w\sin(\psi - \gamma + \delta_s) - u\sin\delta_s) \quad (4)$$

On the other hand, the water generates a hydrodynamic force on the rudder which is equal to:

$$f_r = p_5 u\sin\delta_r \quad (5)$$

For simplicity reasons, we will assume here that the force friction applied to the boat depends on u^2 and it is equal to $-p_2u^2$ [4].
According to Newton's second law of motion in the (b-frame), we have:

$$p_9\dot{u} = f_s\sin\delta_s - f_r\sin\delta_r - p_2u^2 \quad (6)$$

The forces acting on the sailboat rotation are f_s , f_r and an angular friction force $-p_3r$. Therefore, the Newton's second law of motion is given by:

$$p_{10}\dot{r} = d_sf_s - d_rf_r - p_3r \quad (7)$$

By introducing

$$d_s = p_6 - p_7\cos\delta_s \quad (8)$$
$$d_r = p_8\cos\delta_r$$

equation (7) becomes:

$$p_{10}\dot{r} = (p_6 - p_7\cos\delta_s)f_s - p_8\cos\delta_r f_r - p_3r \quad (9)$$

Therefore, the state equations which describe the kinematics of the boat with three degrees of freedom are:

$$\begin{cases} \dot{x} = u\cos\psi + V_C\cos\varphi \\ \dot{y} = u\sin\psi + V_C\sin\varphi \\ \dot{\psi} = r \\ \dot{\delta_s} = u_1 \\ \dot{\delta_r} = u_2 \\ \dot{u} = (f_s\sin\delta_s - f_r\sin\delta_r - p_2u^2)/p_9 \\ \dot{r} = ((p_6 - p_7\cos\delta_s)f_s - p_8f_r\cos\delta_r - p_3r)/p_{10} \end{cases} \quad (10)$$

This differential equation system is highly nonlinear, it has the following form; $\dot{X} = f(X, U)$
With:
$X = (x\ y\ \psi\ \delta_s\ \delta_r\ u\ r)^T$ the state vector, and
$U = \begin{pmatrix} \dot{\delta_s} \\ \dot{\delta_r} \end{pmatrix}$ the system input.

III. AUTOPILOT DESIGN FOR THE SAILBOAT

Our goal is to design an autopilot capable of autonomously bringing the sailboat to a desired ocean position (x_d, y_d). Generally, such autopilot is composed of two regulators: a low-level regulator and a high-level regulator. The first one controls the heading and the sail opening angle. The second one acts as a setpoint generator of two variables: the desired opening angle of the sail $w_1 = \delta_s{}^{ref}$ and the desired boat heading $w_2 = \psi^{ref}$ that will guide the sailboat to its destination. These two regulators have various inputs, such as the wind direction and speed, the sea current, the system state space and the desired position. Fig.3 shows a block diagram of the proposed autopilot. In this study, we will focus on the low-level regulator only. Regarding the set-point generator, we will use the trajectory planning proposed in [5] with minor improvements.

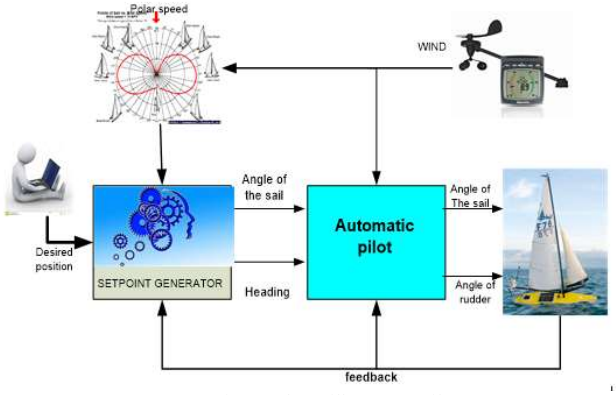

Fig. 2. The sailboat autopilot

The mathematical model obtained (10) is strongly nonlinear. In fact, the state vector is of dimension seven. According to the flatness theory [8], the vector $Y = (\delta_s, \psi)^T$ is a flat output and consequently the system is flat.

ISSN 2356-5608

The sliding mode control design involves two steps: the selection of a sliding surface in the state/error space on which motion should be restricted, called the switching function, and the synthesis of a control law which makes the selected sliding surface attractive.

A. Selection of the sliding surface

In order to apply a feedback linearization method, the output vector was differentiated three times for ψ and once for δ_s. So, we have:

$$\dot{\delta}_s = A_{11}(X)u_1 + A_{12}(X)u_2 + B_{11}(X) \quad (11)$$

With:

$$A_{11}(X) = 1$$
$$A_{12}(X) = 0$$
$$B_{11}(X) = 0$$

The relative degree of the differential equation (11) is equal to one so the chosen sliding surface is given by

$$S_1 = e_1 \quad (12)$$

Where

$e_1 = w_1 - \delta_s$ represents the error on the sail opening angle.

From (10), we extract the following yaw/heading sub dynamics:

$$\dot{\psi} = r \quad (13)$$
$$\ddot{\psi} = ((p_6 - p_7\, cos(\delta_s))f_s - p_8\, cos(\delta_r)\, f_r - p_3 r)/p_{10}$$

With $\psi \in [-\pi, \pi]$.

we derive another time ψ so, we obtain:

$$\dddot{\psi} = A_{21}(X)u_1 + A_{22}(X)u_2 + B_{21}(X) \quad (14)$$

With:

$$A_{21}(X) = \frac{p_7 f_s \sin\delta_s}{p_{10}} + \frac{p_4(p_7\cos\delta_s - p_6)(V_w\sin(\psi+\delta_s) + u\cos\delta_s)}{p_{10}}$$

$$A_{22}(X) = \frac{p_8(f_r\sin\delta_r - p_5 u(\cos\delta_r)^2)}{p_{10}}$$

$$B_{21}(X) = -\frac{p_3\dot{r}}{p_{10}} + \frac{p_4(p_7\cos\delta_s - p_6)(V_w u\sin(\psi+\delta_s) + \dot{u}\sin\delta_s)}{p_{10}} - \frac{p_5 p_8 \dot{u}\sin\delta_r\cos\delta_r}{p_{10}}$$

The relative degree of the differential equation (14) is equal to 3.

So, the chosen sliding surface is given by:

$$S_2 = \lambda_1 e_2 + \lambda_2 \dot{e_2} + \lambda_3 \ddot{e_2} \quad (15)$$

with $e_2 = w_2 - \psi$ the heading error of the vessel.

The coefficients $\lambda_1, \lambda_2, \lambda_3$ are chosen by pole placement method: $\lambda_1 = 1; \lambda_2 = 2; \lambda_3 = 1$

Thereafter, the sliding surface S, which allows the system to converge to the desired state, is written in the form:

$$S = \begin{pmatrix} S_1 \\ S_2 \end{pmatrix} = \begin{pmatrix} e_1 \\ e_2 + 2\dot{e_2} + \ddot{e_2} \end{pmatrix} \quad (16)$$

B. Synthesis of the control law

According to the sliding-mode control theory, we have

$$U = \begin{pmatrix} u_1 \\ u_2 \end{pmatrix} = U_{eq} + U_{cor} \quad (17)$$

where:

$U_{eq} = \begin{pmatrix} u_{1eq} \\ u_{2eq} \end{pmatrix}$ represents the equivalent control. It makes the derivative of the sliding surface equal zero in order to stay on the sliding surface.

$U_{cor} = \begin{pmatrix} u_{1cor} \\ u_{2cor} \end{pmatrix}$ is the corrective control letting the system to compensate the deviations from the sliding surface.

U_{eq} is the solution of the equation system (18):

$$\begin{cases} \dot{S} = \begin{pmatrix} \dot{S}_1 \\ \dot{S}_2 \end{pmatrix} = \begin{pmatrix} 0 \\ 0 \end{pmatrix} \\ U = U_{eq} \end{cases} \quad (18)$$

In other words,

$$-A(X)U_{eq} - B(X) - C(X) = 0$$
$$U_{eq} = -A^{-1}(X)(B(X) + C(X)) \quad (19)$$

This relation is verified if the matrix *A(X)* is invertible.

With

$$A(X) = \begin{pmatrix} A_{11}(X) & A_{12}(X) \\ A_{21}(X) & A_{22}(X) \end{pmatrix}$$
$$B(X) = \begin{pmatrix} B_{11}(X) \\ B_{21}(X) \end{pmatrix}$$
$$C(X) = \begin{pmatrix} C_{11}(X) \\ C_{21}(X) \end{pmatrix} = \begin{pmatrix} 0 \\ \dot{\psi} + 2\ddot{\psi} \end{pmatrix}$$

Let us now determine the singularities of the matrix $A(X)$.

By calculating the expression of $\det(A(X))$, we can show that we have a singularity when this quantity is equal to zero, in other words:

$$\det(A(X)) = 0$$

Then $u = 0$ or $\delta_r = \frac{\pi}{4} + k\frac{\pi}{2}$

This configuration corresponds to a singularity that should be avoided. Hence, the maximum rudder angle will be set to ${\delta_r}^{max} = \frac{\pi}{3}$.

For a scalar function f we denote $\tilde{f}$ the following vectoriel function:

$$\tilde{f}: \Re^2 \to \Re^2 \quad (20)$$
$$\begin{pmatrix} a \\ b \end{pmatrix} \to \tilde{f}\begin{pmatrix} a \\ b \end{pmatrix} = \begin{pmatrix} f(a) \\ f(b) \end{pmatrix}$$

Thus, the expression of the corrective control function U_{cor} is calculated by the resolution of the following equation:

$$\dot{S} = -K\widetilde{sign}(S) \quad (21)$$

where K is a positive design constant.

Or, we have

$$\begin{cases} \dot{S} = -A(X)U - B(X) - C(X) \\ U = U_{eq} + U_{cor} \\ U_{eq} = -A^{-1}(X)(B(X) + C(X)) \end{cases} \quad (22)$$

Therefore, using (21) and (22) we get:

$$U_{cor} = A^{-1}(X)K\widetilde{sign}(S) \quad (23)$$

As a consequence, the control expression is given by:

$$\begin{aligned} U &= U_{eq} + U_{cor} \\ &= -A^{-1}(X)(B(X) + C(X)) + A^{-1}(X)K\widetilde{sign}(S) \\ &= A^{-1}(X)(K\widetilde{sign}(S) - B(X) - C(X)) \end{aligned} \quad (24)$$

ISSN 2356-5608

proof

Let the candidate Lyapunov function be defined by:

$$V = \frac{1}{2}S^T S \tag{25}$$

To ensure the stability and attractiveness of the sliding surface of the control law developed, it is sufficient that $\dot{V} < 0$.

We have

$$\begin{aligned}\dot{V} &= \frac{1}{2}\left(S^T\dot{S} + \dot{S}^T S\right)\\ &= \frac{1}{2}\left(-S^T K\widetilde{sign}(S) - K(\widetilde{sign}(S))^T S\right)\\ &= -K(|S_1| + |S_2|) < 0\end{aligned} \tag{26}$$

So, the asymptotic convergence of the trajectory to the sliding surface is proven.

To reduce the chattering effect, the "signum" function was replaced with an "arc-tangent "function, in order to avoid actuators (rudder and sail) strain and obtain a smooth control behaviour, therefore, we obtain:

$$U = A^{-1}(X)\left(\left(\frac{2}{\pi}\widetilde{\tan}^{-1}\left(K\frac{\pi}{2}S\right)\right) - B(X) - C(X)\right) \tag{27}$$

This low-level regulator generates the control laws $U = \begin{pmatrix}u_1\\ u_2\end{pmatrix}$ regulate the boat heading and the sail opening angle using the sliding mode method. According to the desired position (x_d, y_d), measured heading ψ and wind data the high-level regulator which is inspired from [5] will generate the desired heading $w_2 = \psi^{ref}$ and the desired sail opening angle $w_1 = {\delta_s}^{ref}$.

As we know, if the boat heading is too close to the wind direction, the sail will be luffing ("flapping") in the breeze and cannot generate an aerodynamic force, only making noise like a flag. Different sailboats, have different performance characteristics. These characteristics depend on such variables as sail area, boat mass, hull and keel design.

The polar diagram of a sailboat is the set of all pairs (ψ, u) that can be reached by the sailboat when it navigates. The area of direction that cannot be reached is called a no-go-zone. The size of the no-go zone (no-go- angle) will differ based on the performance characteristics of the particular sailboat.

In case that the boat is up the wind ($\gamma = \pi + \psi$), to avoid the no-go-zone, the high-level regulator generates desired heading

$$\psi^{ref} = \frac{-2\pi}{3} + \gamma \quad \text{and} \quad \psi^{ref} = \frac{2\pi}{3} + \gamma \tag{28}$$

letting the boat tack[2] and reach its destination with maximum speed according to the used boat polar diagram (see Appendix C). When the desired position is located on the south of the boat position, the desired heading given by the high-level regulator which is defined by $atan2$[3] function equal to

$$\psi^{ref} = atan2(y - y_d, x - x_d) \tag{29}$$

Using the sailboat heading ψ the desired sail opening angle is given by (Fig.3):

$${\delta_s}^{ref} = \pi\left[-\frac{\psi}{2\pi} + \frac{1}{2}\right] + \frac{\psi}{2} \tag{30}$$

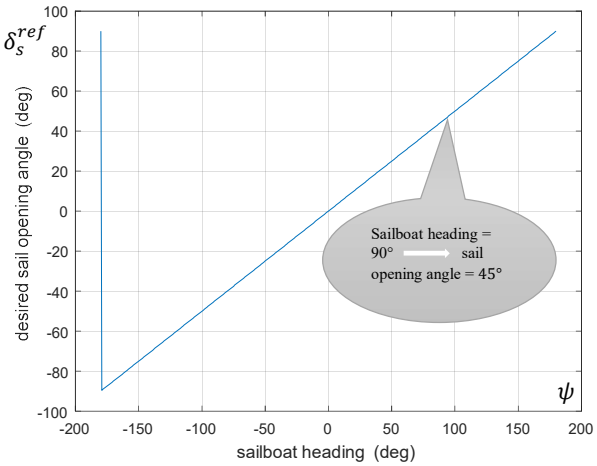

Fig.3. Desired sail opening angle function

IV. SIMULATION

In order to validate the control law developed in this work, the overall system was simulated.

During this simulation, the wind is blowing from the north ($\gamma = \pi$) and its speed equal to 10 m/s. It is indicated by a red arrow (see Fig.6 and Fig.7).

The controller (27) is tuned with $K = 3.5$.

In order to visualize the behaviour of the sailboat facing the wind and down the wind also the robustness of the proposed control law, we have chosen two desired way-point, the first one is located in the south east of the initial position (0,0) and the second one is situated on the north east of the initial position (0,0). Both simulations were started with initial values.

$$X(t = 0) = (0\ 0\ -45°\ 67.5°\ 3.9°\ 8\ 0)^T$$

- The first simulation result represented in Fig.4, shows that the boat goes directly to the desired position which is located in the south east of the initial boat's position.
- Fig.5 shows the path followed by the sailboat during the second simulation. The boat performs the tacking manoeuvre when it is facing the wind. The simulation results show that there is a good synchronization between the rudder and the sail control (Fig.6 and

[2] The sailboat tacks, that is sails on alternating sides of the wind and therefore advances towards the wind. This is the most complex case, testing the interaction between all parts of the model, especially rudder and sail forces.

[3] $atan2(y, x) \in [-\pi, \pi]$ is the four-quadrant inverse tangent.

ISSN 2356-5608

Fig.7) in order to contribute to the direction of the wind that isn't convenient for sailboats.

- Fig.8 show that $\psi(t)$ eventually converges to the desired heading $\psi^{ref}(t)$ with an error $\psi^{ref}(t) - \psi(t) \approx 0$

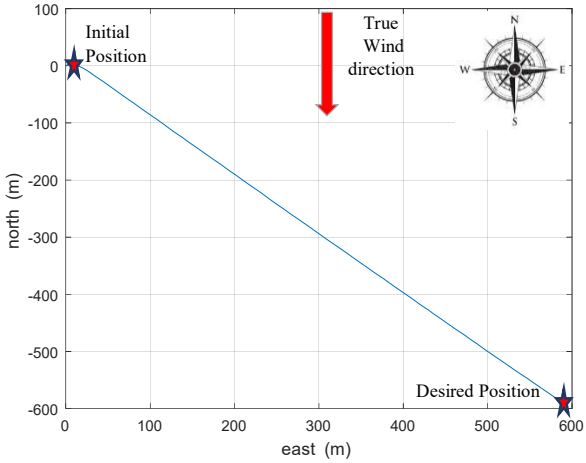

Fig. 4. Path taken by the sailboat $(x_d = 600, y_d = -600)$

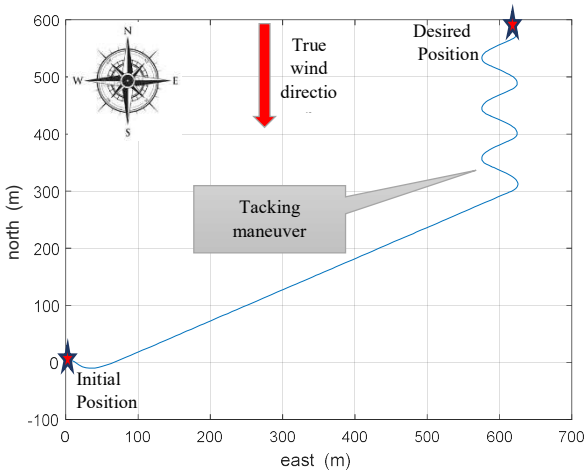

Fig. 5. Path taken by the sailboat $(x_d = 600, y_d = 600)$

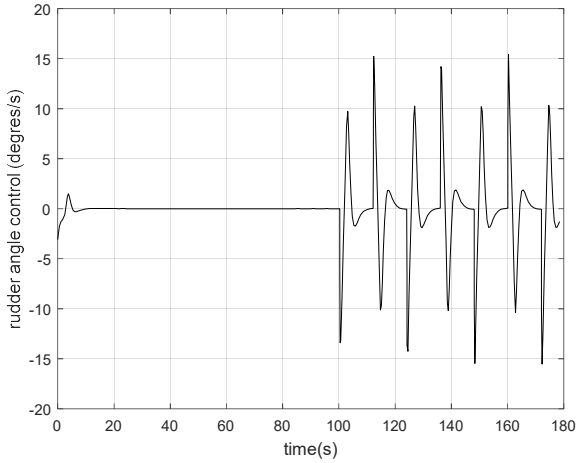

Fig.6. Time evolution of the rudder angle control

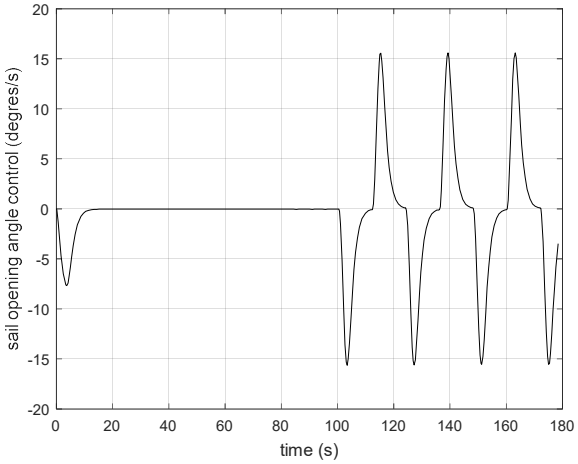

Fig.7. Time evolution of the sail opening angle control

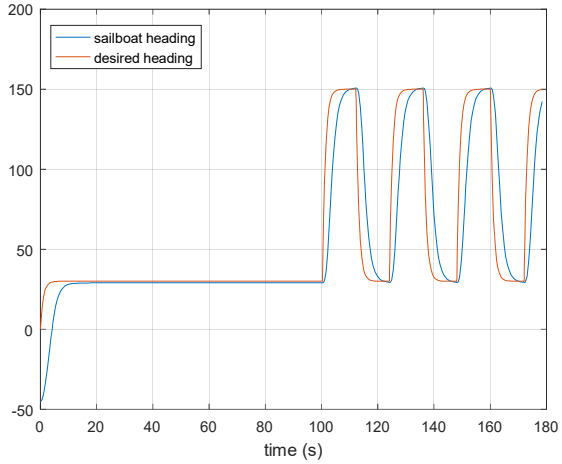

Fig.8. Time evolution of the desired heading ψ^{ref} and the sailboat heading ψ

V. CONCLUSION

In this paper, a 3-DOF mathematical model describing the dynamic motion of a sailboat was presented. This model is simple and contains several approximations such as the neglect of drifting effect and rolling motion but it is an adequate model in order to apprehend the sailboat dynamic motion in the horizontal plane. The sliding mode control approach is employed to perform heading and sail opening angle control for the sailing boat.

The simulation results show that the used control technique gives good results in terms of regulation but with relatively small errors, this technique has also some disadvantages, such as the chattering phenomenon caused by the 'signum' function. However, this problem is solved by applying the 'arc-tangent' function which gives better results in terms of regulation through a smooth control. Futur work in this area is the design of a sailboat autopilot based on sliding mode control applied to the non-linear system without feedback linearization method and the next step a

ISSN 2356-5608

comparison between these two control laws will be discussed.

After the validation of the proposed control law through simulation, the proposed control law will be tested on a real sailboat.

REFERENCES

[1] BRIERE, Yves. Iboat: An autonomous robot for long-term offshore operation. In : Electrotechnical Conference, 2008. MELECON 2008. The 14th IEEE Mediterranean. IEEE, 2008. p. 323-329.

[2] CRUZ, Nuno A. et ALVES, Jose C. Navigation performance of an autonomous sailing robot. In : Oceans-St. John's, 2014. IEEE, 2014. p. 1-7.

[3] ERCKENS, Hendrik, BEUSSER, Gion-Andri, PRADALIER, Cedric, et al. Avalon. IEEE robotics & automation magazine, 2010, vol. 17, no 1, p. 45-54.

[4] JAULIN, Luc et LE BARS, Fabrice. A simple controller for line following of sailboats. In : Robotic Sailing 2012. Springer, Berlin, Heidelberg, 2013. p. 117-129.

[5] JAULIN, Luc. Modelisation et commande dun bateau a voile. In : Proceedings of 3rd Conference Internationale Francophone dAutomatique, Douz, Tunisie. 2004.

[6] JOUFFROY, Jerome. A control strategy for steering an autonomous surface sailing vehicle in a tacking maneuver. In : Systems, Man and Cybernetics, 2009. SMC 2009. IEEE International Conference on. IEEE, 2009. p. 2391-2396.

[7] LAROCHE, Béatrice, MARTIN, Philippe, et PETIT, Nicolas. Commande par platitude. Equations différentielles ordinaires et aux dérivées partielles. 2008.

[8] LEGURSKY, Katrina. A modified model, simulation, and tests of a full-scale sailing yacht. In : Oceans, 2012. IEEE, 2012. p. 1-7.

[9] ROMERO-RAMIREZ, Miguel-Angel. Contribution à la commande de voiliers robotisés. 2012. Thèse de doctorat. Paris 6.

[10] STELZER, Roland, PROLL, Tobias, et JOHN, Robert I. Fuzzy logic control system for autonomous sailboats. In : Fuzzy Systems Conference, 2007. FUZZ-IEEE 2007. IEEE International. IEEE, 2007. p. 1-6.

[11] Treichel, K. and Jouffroy, J. Real-time sail and heading optimization for a surface sailing vessel by extremum seeking control. In 55th International Scientific Colloquium (IWK), Ilmenau, Germany. 2010

[12] Xiao, K., Sliwka, J., and Jaulin, L. A wind-independent control strategy for autonomous sailboats based on voronoi diagram. In Proceedings of CLAWAR 2011 : the 14th International Conference on Climbing and Walking Robots and the Support Technologies for Mobile Machines, pages 109–123. 7, 22

[13] XIAO, Lin et JOUFFROY, Jerome. Modeling and nonlinear heading control of sailing yachts. IEEE Journal of Oceanic engineering, 2014, vol. 39, no 2, p. 256-268.

[14] YANG, Bin, XIAO, Lin, et JOUFFROY, Jerome. A control-theoretic outlook at the no-go zone in sailing vessels. In : OCEANS 2011. IEEE, 2011. p. 1-7.

[15] YEH, Edge C. et BIN, Jenn-Cherng. Fuzzy control for self-steering of a sailboat. In : Intelligent Control and Instrumentation, 1992. SICICI'92. Proceedings., Singapore International Conference on. IEEE, 1992. p. 1339-1344.

[16] GOMES, Luís, SANTOS, Miguel, PEREIRA, Thiago, et al. Model-based development of an autonomous sailing Yacht controller. In : Autonomous Robot Systems and Competitions (ICARSC), 2015 IEEE International Conference on. IEEE, 2015. p. 103-108.

[17] JAULIN, Luc, LE BARS, Fabrice, CLEMENT, Benoît, et al. Suivi de route pour un robot voilier. In : Conférence Internationale Francophone d'Automatique (CIFA2012). 2012. p. 695-702.

Appendix A. VARIABLE DESCRIPTION

Notation	Description
V_w	-wind speed
γ	-wind direction
V_C	-maritime current speed
φ	-maritime current direction
G	-boat's center of gravity
(x, y)	-coordinates of the sailboat's center of gravity
ψ	-heading in the (n-frame)
δ_s	-sail angle in the (b-frame)
δ_r	-rudder angle in the (b-frame)
u	-linear velocity in the (b-frame)
r	-yaw velocity in the (b-frame)
f_s	-aerodynamic force of the wind applied on the sail in the (b-frame)
f_r	-hydrodynamic force of the water applied on the rudder in the (b-frame)
p_1	-boat's drift coefficient
p_2	-water friction
p_3	-water angular friction
p_4	-lift coefficient of the sail
p_5	-lift coefficient of the rudder
p_6	-distance between the mast and the center of the sail
p_7	-distance between the boat's center of gravity and the mast
p_8	-distance between G and the rudder
p_9	-total mass of the boat (including the added-mass)
p_{10}	-moment of inertia

Appendix B. SURGE, SWAY AND YAW MOTION

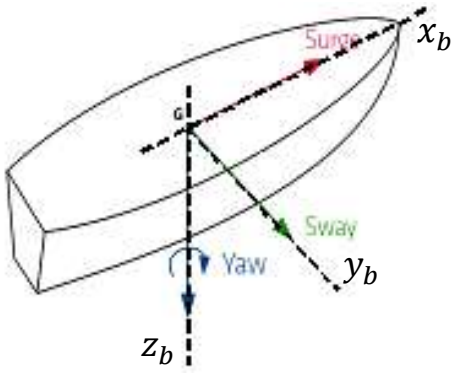

Appendix C. The used sailboat polar diagram

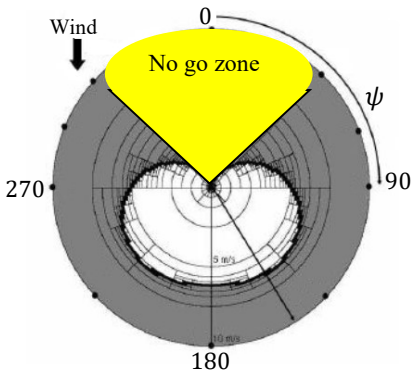

ISSN 2356-5608